

# Variations of coronary sinus tributaries among patients undergoing cardiac resynchronisation therapy

B. Gach-Kuniewicz<sup>1</sup>, G. Goncerz<sup>1</sup>, D. Ali<sup>1</sup>, M. Kacprzyk<sup>2</sup>, M. Zarzecki<sup>1</sup>, M. Loukas<sup>3, 4</sup>, J. Walocha<sup>1</sup>, E. Mizia<sup>1</sup>

<sup>1</sup>Department of Anatomy, Jagiellonian University Medical College, Krakow, Poland

<sup>2</sup>Department of Electrophysiology, Institute of Cardiology, Jagiellonian University Medical College, Krakow, Poland

<sup>3</sup>Department of Anatomical Sciences, St. George's University, Grenada, West Indies

<sup>4</sup>Department of Anatomy, Varmia and Mazury University, Olsztyn, Poland

[Received: 19 February 2022; Accepted: 7 April 2022; Early publication date: 28 April 2022]

**Background:** In cardiac resynchronisation therapy (CRT), the coronary venous system is used for left ventricular pacing electrode placement. Despite the well-known anatomy of the coronary sinus and its tributaries, heart failure patients' remodelled and enlarged left ventricles may impede the successful lead placement because of acquired anatomical obstacles.

**Materials and methods:** Fifty-five patients qualified for CRT treatment were divided into ischaemic and non-ischaemic cardiomyopathy. Forty-four control groups without heart failure underwent dual-source computed tomography (CT). Rendered reconstructions of cardiac coronary systems were compared.

**Results:** The presence of main tributaries was comparable in all groups. The left marginal vein, small cardiac vein, and oblique vein of the left atrium were present in 63%, 60%, and 51% of the hearts in all the groups. CRT referred CTs had significantly longer distances between posterior and lateral cardiac veins over the left ventricle ( $p < 0.05$ ), wider angles of tributaries ( $p = 0.03$ ), and smaller lumen of coronary sinus ( $p = 0.03$ ). In the non-ischaemic group, the posterior interventricular and great cardiac veins are more extensive than in the control group. Age-related analysis of vessel size shows a moderate correlation between age and diminishing mean vessel size in all the groups studied.

**Conclusions:** The general structure of the coronary heart system is consistent in patients with and without heart failure. The variance of the general structure, or the presence of adequate veins, is an individual variation. The use of CT and analysis of the coronary veins allow better planning of the CRT-D implantation procedure and may reduce the risk of ineffective left ventricular electrode implantation. (Folia Morphol 2023; 82, 2: 282–290)

**Key words:** coronary sinus, resynchronization therapy, heart failure

Address for correspondence: B. Gach-Kuniewicz, MD, Department of Anatomy, Jagiellonian University Medical College, ul. Kopernika 12, 31–034 Kraków, Poland, tel/fax: +48 12 422 95 11, e-mail: bgkuniewicz@gmail.com

This article is available in open access under Creative Common Attribution-Non-Commercial-No Derivatives 4.0 International (CC BY-NC-ND 4.0) license, allowing to download articles and share them with others as long as they credit the authors and the publisher, but without permission to change them in any way or use them commercially.

## INTRODUCTION

The coronary venous system consisting of the coronary sinus (CS) and its tributaries contributes to most venous drainage from the heart muscle. The great cardiac vein (GCV), middle cardiac vein (MCV)/posterior interventricular vein (PIV), and small cardiac vein (SCV), in addition to the left marginal vein (LMV), the posterior vein of the left ventricle (PVLV), and oblique vein of the left atrium (OVLA), also known as the vein of Marshall (VoM), constitute the most constant tributaries of the CS [8, 13, 18, 20, 21, 24, 27].

The coronary system is often used during invasive transcatheter procedures, such as radiofrequency ablation, biventricular pacing, retrograde cardioplegia administration, or mitral annuloplasty. Furthermore, the CS and GCV are relevant in almost every electrophysiology procedure and are often used as landmarks for safe transseptal punctures [11]. In addition, consideration is given to the use of the MCV for the placement of left ventricular leads and ablation of posterior epicardial accessory pathways or the treatment of epicardial ventricular arrhythmias. Meanwhile, the PVLV or LMV, both of which drain the lateral wall of the left ventricle (LV), are often the target for left ventricular or biventricular pacing [6, 10, 19].

Cardiac resynchronisation therapy (CRT) is a well-established treatment for patients with dilation and systolic dysfunction of the LV, and electrocardiographic evidence of intraventricular conduction delay. The reason for left ventricular dilation may be advanced ischaemic heart disease or there may be non-ischaemic reasons. Resynchronisation therapy requires the insertion of right and left ventricular leads to resynchronise ventricular contraction. For the successful pacing of the LV and the success of epicardial pacing, the use of one of the posterolateral tributaries of the CS is imperative [1, 4, 8, 21]. Unfortunately, 30–40% of patients do not respond adequately to CRT [17]. Trespassing through the Thebesian and Vieussens valve is one of the determinants of this response [14, 32].

The successful left ventricular pacing depends on the coronary system constitution and the highly variable anatomy of the CS and its tributaries. The important fact is that CRT is required for selected patients obtaining physical and imaging requirements for heart failure (HF) improvements without aetiology differentiation. We believe that blood flow reduction in ischaemic aetiology reduces the volume of coronary

veins, impeding successful electrode placement. In contrast, non-ischaemic aetiology will change only the architecture of the coronary system.

Clinical experience, manual skills, and knowledge of the coronary venous system anatomy are necessary for successful CS cannulation and reaching the desirable vein. Although CS anatomy is well-known, hearts with LV enlargement and cardiomyopathy anatomically differ from general anatomy. Remodelling the LV myocardial scar may change the size of the CS tributaries, angulations, constrict or close the existing vessels, and impede the invasive procedure, making it more challenging or even impossible to perform [25]. Therefore, this study aims to evaluate the CS tributaries anatomy in ischaemic and non-ischaemic cardiomyopathy vs. non-HF venous anatomy.

## MATERIALS AND METHODS

This study was approved by the local ethics committee [NB.060.1.26.2021]. The study protocol conformed to the ethical guidelines of the 1975 Declaration of Helsinki. The methods were executed per the approved guidelines.

### Study populations

This study included 55 consecutive patients (mean age  $65 \pm 12$  [35–82] years, 11 women [20%]) with HF, considered to CRT treatment, who underwent dual-source computed tomography (CT).

The designation of patients from the HF group, according to aetiology, was 29 (52%) to ischaemic cardiomyopathy (ischaemic HF) and 26 (48%) to non-ischaemic cardiomyopathy (non-ischaemic-HF). From the non-ischaemic HF group, 22 were idiopathic dilated cardiomyopathy, 1 hypertrophic, 1 post-infectious, 2 tachy-cardiomyopathy. Five patients from the HF group had implantable cardioverter-defibrillator and 2 had pacemakers.

For more accurate anatomical comparison we included 44 non-HF patients from the control group (mean age  $61.9 \pm 13.7$  years [20–91] 24 women [54.5%]), who underwent CT evaluation of coronary artery disease ( $n = 20$ ) and pulmonary veins before cryoballoon ablation ( $n = 24$ ).

Descriptions of further clinical details of patients from each group are shown in Table 1.

### CT-protocol

Before each cardiac CT examination, every patient had a pulse check. If a patient's heart rate was over

**Table 1.** Characteristics of the study population

	Ischaemic-HF (n = 29)	Non-ischaemic-HF (n = 26)	Non-HF (n = 44)
Sex: female	3 (10.3%)	9 (34.6%)	24 (54.5%)
Age ( $\pm$ SD) [year]	66.23 $\pm$ 10.72 (35–82)	62.2 $\pm$ 12.97 (31–81)	61.9 $\pm$ 13.7 (20–91)
Ejection fraction [%]	24.55 $\pm$ 6.47 (35–10)	24.88 $\pm$ 7.14 (35–15)	54.2 $\pm$ 9.1 (44–72)
NYHA	II–III	II–III	I
QRS duration [ms]	140 $\pm$ 23 (120–160)	146 $\pm$ 36 (124–174)	91 $\pm$ 15 (80–110)
Hypertension	25 (86.2%)	18 (69.2%)	36 (81%)
Diabetes type 2	12 (41.4%)	6 (23.1%)	12 (27%)
Hypercholesterolaemia	28 (96.5%)	13 (50%)	26 (59%)
Chest pain	18 (62.1%)	10 (38.5%)	30 (68%)
Dyspnoea	24 (82.8%)	19 (73.1%)	30 (68%)
Atrial fibrillation	10 (34.5%)	7 (26.9%)	24 (54.5%)
Atrio-ventricular block	3 (10.3%)	4 (15.4%)	0 (0%)

HF — heart failure; NYHA — New York Heart Association; SD — standard deviation

70 bpm, 10 mg or 40 mg of propranolol or 40 mg verapamil was administered, according to medical indications. A dual-source CT scanner (Somatom Definition, Siemens, Erlangen, Germany) and the contrast-enhanced electrocardiogram (ECG)-retrospectively gated image acquisitions were performed during an inspiratory breath-hold. The imaging parameters for the dual-source CT were a tube voltage of 100–120 kV and an effective tube current of 350–400 mA. The collimation and temporal resolution revealed  $2 \times 32 \times 0.6$  mm and 165 ms. Determination of the arrival time of the contrast agent to the ascending aorta at the level of the carina employed the use of the test bolus method (volume of 15 mL contrast agent, followed by 20 mL saline). The procedure works by injecting the contrast agent at the dose of 1.0 mL/kg and a rate of 5.5 mL/s followed by a 40 mL saline chaser at the same rate range. The acquisition delay was the time of maximum density of the ascending aorta in the test bolus with an additional 6 s of delay. Image reconstruction using B26f and B46f kernel and an image matrix of  $512 \times 512$  pixels allowed for an assessment of the best quality image reconstructions after the multiphase reconstruction (from 10% to 100%). Uses of a dedicated workstation (Aquarius, TeraRecon, San Mateo, United States) by an experienced radiologist allowed for the performance of post-processing and study evaluation. Multiplanar (MPR) and volume-rendered technique (VRT) reconstructions allowed identification of CS ostium in Ludinghausen modifications, number, and variety of veins over LV, distances, and angles between branches of CS.

### Anatomic observation

The anatomy of the CS and its tributaries was studied and identified on the volume-rendered reconstructions, and the course of the veins was evaluated in three orthogonal planes using multiplanar reformatting [7]. The categorization of each heart used one of the three types proposed by Von Ludinghausen [26].

First, the ostium of the sinus was identified from the right atrium, using multiplanar reformatting for measurements in two directions [28]. The subsequent examination considered the presence of each CS tributary (SCV, MCV, PVLV, LMV, VoM, and AIV). In addition to the assessments of the 5.1 F (1.7 mm) and LV-electrode cannulation of each tributary, the verification of the presence of the Vieussens valve and the distance between the ventricular tributaries was measured on volume-rendered reconstructions (Fig. 1).

### Statistical analysis

The presentation of data is as follows: (1) mean values with the corresponding standard deviations and ranges; and/or (2) determining percentages. To verify a relative homogeneity of variance, we performed Levene's tests. The Student's t-tests and the Mann-Whitney U tests were used for statistical comparisons. Additionally, qualitative variables were compared using  $\chi^2$  tests of proportions for categorical variables. Statistical analyses using StatSoft STATISTICA 13.1 software for Windows (StatSoft Inc., Tulsa, OK, USA) enable the detection of a moderate correlation ( $r = 0.4$ ), for 80% power with a 5% significance level (two-tailed;  $\alpha = 0.05$ ;  $\beta = 0.2$ ). The statistical significance was set at a p-value lower than 0.05.

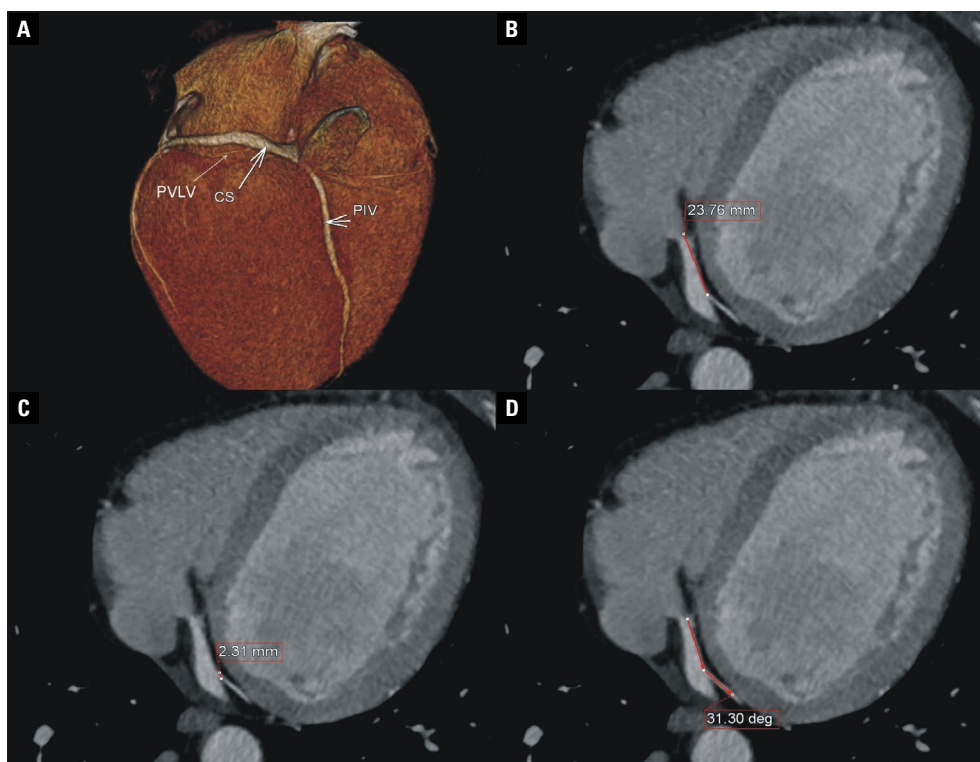


**Figure 1.** Coronary veins anatomy (A) and quantitative analysis of distance from coronary sinus (CS) ostium (B), diameter (C), angle (D) of insertion using multiplanar and volume rendered technique reconstructions; PVLV — posterior vein of the left ventricle; PIV — posterior interventricular vein.

## RESULTS

### Study population

The imaging studies to visualise the cardiac venous system were performed in all patients in all groups. The CS, PIV, PVLV, and AIV were present in all patients. There is an observation of the LMV, in ischaemic-HF/nonischaemic-HF/control group in the 21, 15 and 26 (72.4%, 57.7%, 59.1%) hearts, OVLA in the 10, 11 and 30 (34.5%, 42.3%, 68.2%) hearts, and SCV in the 15, 19 and 25 (51.7%, 73.1%, 56.8%) hearts, respectively.

Anatomical variants (proposed by Von Ludwighausen) vary between the groups. In ischaemic-HF most common variant was with SCV continuity into CS (variant 1) (58.6%  $p < 0.05$ ). In non-ischaemic-HF and non-HF with separate SCV presented with PIV connected to the crus-cordis (variant 2). The third variant with PIV disconnected to the CS was the rarest, with a presence from 6.9% in ischaemic-HF to 11.4%, 11.5% in non-HF, and non-ischaemic-HF.

The OVLA (vein of Marshall) was distinguishable in 12/44 (27.3%) in the non-HF ( $p = 0.18$ ) group compared to 4/29 (13.8%) and 6/26 (19.2%) in both HF

groups. A rare appearance of the Vieusens valve appears in approximately 20% of all the groups. Table 2 summarizes detailed information of anatomical observations.

### Quantitative data

The distances between the main tributaries draining venous blood from LV, angles, and diameters of specific branches demonstrate observable differentials. While most values are not statistically significant between the groups in general summaries, some measurements conduct important differences. PVLV-LMV interspace and angle of PIV in both HF vs. non-HF groups ( $p < 0.005$ ) reveal essential discrepancies between the distances. The mean distance in the non-HF group was  $35.67 \pm 13.53$  mm, while in non-ischaemic-HF,  $46.56 \pm 17.15$  to  $47.54 \pm 10.98$  mm ( $p = 0.002$ ) in the ischaemic-HF group. The angle of PIV entering CS in HF hearts was significantly bigger —  $110.74 \pm 22.42^\circ$  ( $p = 0.03$ ) in ischaemic-HF and  $116.1 \pm 21.38^\circ$  ( $p = 0.03$ ) in non-ischaemic-HF vs. non-HF group  $98.4 \pm 22.94^\circ$ . Figure 2 presents a summary of vessel displacement.

**Table 2.** Anatomic observations. Quantitative analysis of coronary sinus anatomy and its tributaries

	Ischaemic-HF (n = 29)	Non-ischaemic-HF (n = 26)	Non-HF (n = 44)
Coronary sinus:			
Type 1*	17 (58.6%)	4 (15.4%)	12 (27.3%)
Type 2*	10 (34.5%)	19 (73.1%)	27 (61.4%)
Type 3*	2 (6.9%)	3 (11.5%)	5 (11.4%)
Small cardiac vein	15 (51.7%)	19 (73.1%)	25 (56.8%)
Posterior interventricular vein:			
Posterior vein of left ventricle	S: 4 (14%) M: 25 (86%)	S: 3 (12%) M: 23 (88%)	S: 8 (18%) M: 36 (82%)
Left marginal vein	21 (72.4%)	15 (57.7%)	26 (59.1%)
Vein of Marshall	4 (13.8%)	5 (19.2%)	12 (27.3%)
Viussens valve	6 (20.1%)	4 (15.4%)	8 (18.2%)
Anterior interventricular vein	29 (100%)	26 (100%)	44 (100%)

\*Types refer to von Ludinghausen classification; HF — heart failure; S — single; M — multiple

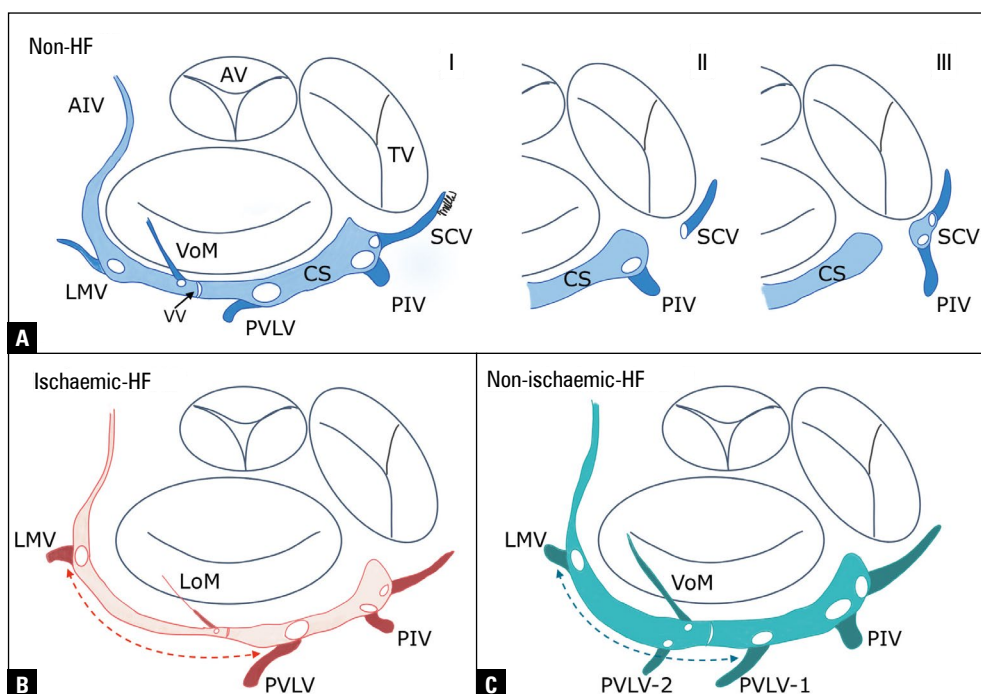


**Figure 2.** Schematic picture of differences between non-HF (blue) group (A) and ischaemic-HF (red) group (B) and non-ischaemic-HF (C); Panel A represents three types of von Ludinghausen modifications I, II and III; AIV — anterior interventricular vein; AV — aortic valve; CS — coronary sinus; HF — heart failure; LMV — left marginal vein; LoM — ligament of Marshall; PIV — posterior interventricular vein; PVLV — posterior vein of left ventricle; SCV — small cardiac vein; TV — tricuspid valve; VoM — vein of Marshall; VV — Vieussens valve.

Then, the separate consideration of differences for each group. In ischaemic-HF vs. non-HF (control group), vessel diameters are generally smaller with statistical significance in AIV diameter (2.64 vs. 3.18 mm,  $p = 0.01$ ). Also, the CS diameter (6.82 vs. 7.84 mm,  $p = 0.03$ ) and CS ostium ( $p = 0.03$ ) are smaller. Such significances do not appear in non-ischaemic-HF

vs. non-HF groups. In non-ischaemic-HF, the differences are opposite. PVI diameter (5.43 vs. 3.9 mm,  $p = 0.01$ ) was significantly larger than non-HF groups, while the CS diameter was bigger, approximately 5 mm. However, this is without statistical significance ( $p = 0.8$ ).

Comparing HF groups, PIV diameter is significantly broader in nonischaemic-HF vs. ischaemic (5.43 vs.

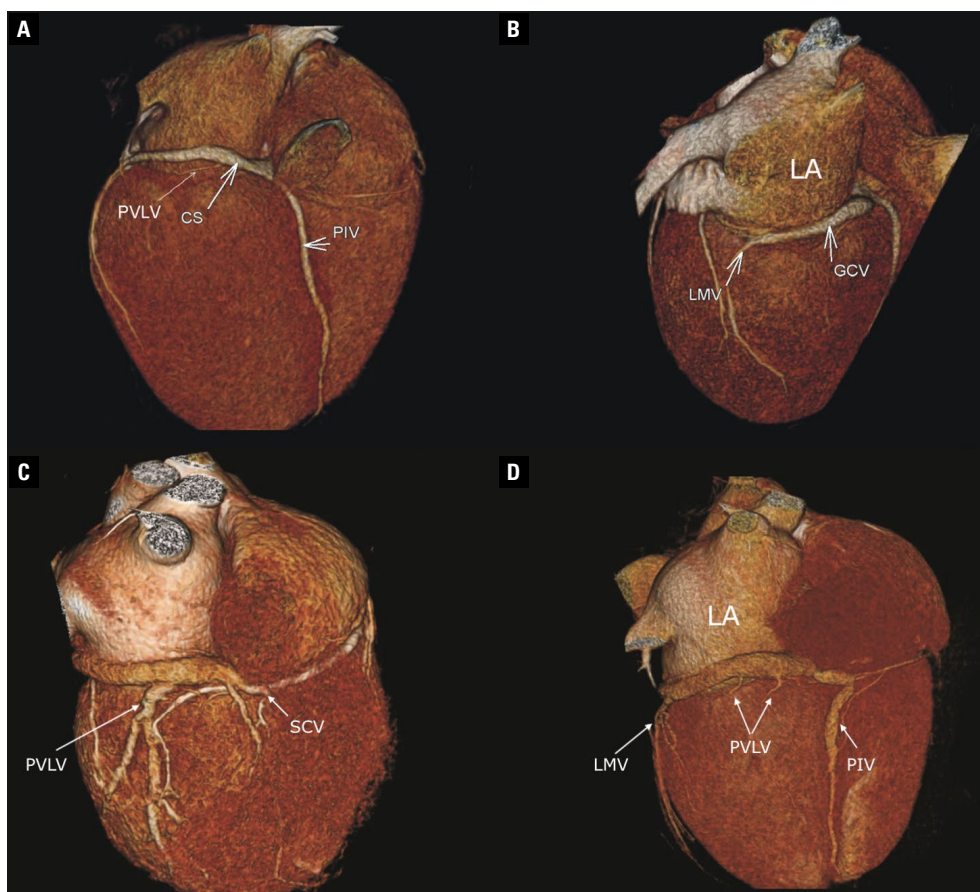


**Figure 3.** Rendered reconstructions of coronary sinus (CS) with tributaries; **A, B.** In ischaemic heart failure; **C, D.** In non-ischaemic heart failure; GCV — great cardiac vein; LA — left atrium; LMV — left marginal vein; PIV — posterior interventricular vein; PVLV — posterior vein of left ventricle; SCV — small cardiac vein.

4.33 mm,  $p = 0.04$ ), as is the CS diameter (8.3 vs. 6.82 mm,  $p = 0.03$ ). The presentation of differentials for each HF group is on the volume-rendered reconstructions (Fig. 3).

Results demonstrate moderate correlations between the patient's age and AIV diameter in ischaemic-HF ( $r = 0.56$ ,  $p = 0.21$ ) and PIV angle in non-ischaemic-HF ( $r = 0.40$ ,  $p = 0.6$ ). Furthermore, correlations with left ventricular ejection fraction (LVEF) only present in ischaemic-HF between SCV diameter ( $r = 0.55$ ,  $p = 0.8$ ) and LMV angle ( $r = 0.43$ ,  $p = 0.5$ ). None from correlations because sample size reached statistical significance.

Finally, the attainable vessels were counted for possible LV lead placement. For accessible vessels for the CRT, the size of 5.1 F (1.7 mm) and angle is less than  $60^\circ$  [2] are considered. The size over 1.7 mm was found in 23/26 PVLV and 10/15 LMV in non-ischaemic-HF and 28/29 and 16/21 in ischaemic-HF. The tributaries' ostium angles less than  $60^\circ$  advanc-

ing cannulation were found in 13/26 PVLV and 10/15 LMV in nonischaemic-HF and 14/29 and 11/21 in ischaemic-HF. The only correlation in the  $\chi^2$  test was found in PVLV diameter for ischaemic-HF favouring implantation  $p = 0.02$ .

Table 3 summarizes the quantitative data.

## DISCUSSION

Cardiac resynchronisation therapy provides HF improvement and an effective increase in LVEF only in 70% of the patients. For years, the statement that nearly one-third of CRT patients do not respond to resynchronization therapy has become general knowledge. It is discussed and partially accepted without questioning the reasons [2]. Besides optimal programming of the CRT device, the anatomical structure of the coronary system plays the crucial role. Remodelled heart muscle with venous drainage may differ from a healthy one, and the aim of that study emphasizes such discrepancies.

**Table 3.** Anatomic observations. Qualitative analysis of diameters, distances and angles of coronary sinus and its tributaries

	Ischaemic-HF (n = 29)	Non-ischaemic-HF (n = 26)	Non-HF (n = 44)
Ostium CS antero-posterior diameter	9.26 ± 4.02	9.8 ± 4.25	11 ± 4.3
Ostium CS superior-inferior diameter	14.94 ± 5.6 (p = 0.03)*	16.24 ± 6	18.36 ± 7.74
SCV diameter [mm]	1.37 ± 0.65	2.19 ± 1.3	1.5 ± 0.75
PIV diameter [mm]	4.33 ± 1.88 (p = 0.04)**	5.43 ± 2.03 (p = 0.01)*	3.9 ± 1.78
PVLV diameter [mm]	3.35 ± 1.17	3.15 ± 1.17	3.1 ± 1.46
LMV diameter [mm]	2.3 ± 1.04	2.62 ± 1.04	2.72 ± 1.27
GCV diameter [mm]	6.82 ± 1.46 (p = 0.03)*	8.3 ± 3.14 (p = 0.03)**	7.84 ± 2.49
AIV diameter [mm]	2.64 ± 0.83 (p = 0.02)**	2.86 ± 1.45	3.17 ± 0.98
CS ostium PIV distance [mm]	4.21 ± 2.68	3.12 ± 2.46	3.25 ± 3.32
PIV–PVLV distance [mm]	24.33 ± 10.43	27.4 ± 15.75	28.32 ± 15.31
PVLV–LMV distance [mm]	47.54 ± 10.98 (p = 0.002)*	46.56 ± 17.15 (p = 0.005)	35.67 ± 13.53
PIV angle [°]	110.74 ± 22.42 (p = 0.03)*	116.1 ± 21.38 (p = 0.03)*	98.4 ± 22.94
PVLV angle [°]	54.56 ± 22.87	61.46 ± 26.04 (p = 0.04)*	50.82 ± 26.94
LMV angle [°]	62 ± 33.54	50.25 ± 20.14	55.39 ± 37.92

\*Statistical significance to control group (non-HF), \*\*statistical significance between ischaemic to non-ischaemic HF; AIV — anterior interventricular vein; CS — coronary sinus; GCV — great cardiac vein; HF — heart failure; LMV — left marginal vein; PIV — posterior interventricular vein; PVLV — posterior vein of the left ventricle; SCV — short cardiac vein

The general structure of the coronary heart system is consistent in patients with and without HF [9, 12, 30]. The variance of the general structure, or the presence of particular veins, is an individual variation [3, 13, 20, 22, 23]. It refers mainly to the prevalence of LMV (from 72.4–57.7%) in all groups. As in VoM, where the occurrence variability is high, and the detection ability is low [15, 33]. When VoM is not visible the structure which is present is the ligament of Marshall (LoM) (Fig. 2C).

Besides the individual arrangement of veins, ventricular remodelling affects the coronary system in HF patients. When analysing individual subgroups, the most significant difference between the coronary system in HF and the control group (non-HF) is the substantial change in the distance between PVLV and LMV (Fig. 2B, C). The average elongation of these distances ranges 12 mm. Apart from the PVLV outlet is variable and often multi-vessel (Fig. 3D). Vein displacement also changes the outlet angles. PIV shifts from the CS outlet further affect the outlet angles. While the distance appears to be statistically insignificant, the change in vessel angle from 98.4° to 110.7° (p = 0.03) indicates a shift in the vessel's outlet relative to the mitral ring. An interesting observation is a change in the diameters of individual vessels — ischaemic-HF heart coronary sinuses demonstrate a reduction in vein diameter (GCV, AIV, CS outlets) when compared with non-HF (p = 0.01). Inversely, these vessels in the nonischaemic-HF group are more extensive

than in the study group, mainly PIV and GCV (p = 0.01). Performing an age-related correlation analysis of vessel size — we found a moderate correlation between the age and mean vessel size in all the groups studied. The Mazur et al. [13] study demonstrates similar observations. Finally, the CS outlet also differs between groups. Assuming application of the S-I (superior–inferior) and A-P (anterior–posterior) dimensions to the ellipse area, it turns out that the CS opening in the ischaemic-HF is significantly smaller than in the control group. It relates to the ischaemic-HF group, in which there was a less frequent observation of the presence of the Thebesian valve [31]. Nevertheless, the coronary venous system is fragmentary stenosed in patients with ischaemic-HF, while significantly widened in individual segments in nonischaemic-HF concerning the control group — non-HF.

The observed qualitative differences result from changes in the architecture of the heart muscle itself, which cause vessel displacement and changes in ostium angles [5]. Left ventricle dilation determines the displacement change in HF patients. Analysing the possibility of LV electrode placement in PVLV or LMV veins with a 5.1 F LV electrode is likely to be highly successful. According to the lumen size, the possible cannulation ranges from 66–96%; however, the anatomy of the coronary system is not the only determinant of the final location of the electrode. It also depends on the resynchronization response of the LV assessed by the ECG and echocardiography

[16, 20, 29]. Access to the vessels due to the angular departure makes 50% of the vessels easily accessible. Additionally, the change of vessel angles in HF vs. non-HF facilitates cannulation by reducing the departure angles ( $p = 0.02$ ). The use of CT and analysis of the coronary veins allow better planning of the CRT-D implantation procedure and may reduce the risk of ineffective left ventricular electrode implantation.

## CONCLUSIONS

The general structure of the coronary heart system is consistent in patients with and without HF.

The substantial change between HF vs. non-HF hearts is the distance elongation between outlets of veins draining the LV.

In ischaemic-HF hearts the volume of the CS is generally smaller, while in non-ischaemic-HF broader to control group.

The change of vessel angles in HF vs. non-HF facilitates cannulation by reducing the departure angles.

**Conflict of interest:** None declared

## REFERENCES

1. Becker M, Hoffmann R, Schmitz F, et al. Relation of optimal lead positioning as defined by three-dimensional echocardiography to long-term benefit of cardiac resynchronization. *Am J Cardiol.* 2007; 100(11): 1671–1676, doi: [10.1016/j.amjcard.2007.07.019](https://doi.org/10.1016/j.amjcard.2007.07.019), indexed in Pubmed: [18036367](https://pubmed.ncbi.nlm.nih.gov/18036367/).
2. Butter C, Georgi C, Stockburger M. Optimal CRT implantation—where and how to place the left-ventricular lead? *Curr Heart Fail Rep.* 2021; 18(5): 329–344, doi: [10.1007/s11897-021-00528-9](https://doi.org/10.1007/s11897-021-00528-9), indexed in Pubmed: [34495452](https://pubmed.ncbi.nlm.nih.gov/34495452/).
3. Cendrowska-Pinkosz M. The variability of the small cardiac vein in the adult human heart. *Folia Morphol.* 2004; 63(2): 159–162, indexed in Pubmed: [15232770](https://pubmed.ncbi.nlm.nih.gov/15232770/).
4. Gold MR, Auricchio A, Hummel JD, et al. Comparison of stimulation sites within left ventricular veins on the acute hemodynamic effects of cardiac resynchronization therapy. *Heart Rhythm.* 2005; 2(4): 376–381, doi: [10.1016/j.hrthm.2004.12.025](https://doi.org/10.1016/j.hrthm.2004.12.025), indexed in Pubmed: [15851339](https://pubmed.ncbi.nlm.nih.gov/15851339/).
5. Gold MR, Thébault C, Linde C, et al. Effect of QRS duration and morphology on cardiac resynchronization therapy outcomes in mild heart failure: results from the Resynchronization Reverses Remodeling in Systolic Left Ventricular Dysfunction (REVERSE) study. *Circulation.* 2012; 126(7): 822–829, doi: [10.1161/CIRCULATIONAHA.112.097709](https://doi.org/10.1161/CIRCULATIONAHA.112.097709), indexed in Pubmed: [22781424](https://pubmed.ncbi.nlm.nih.gov/22781424/).
6. Habib A, Lachman N, Christensen KN, et al. The anatomy of the coronary sinus venous system for the cardiac electrophysiologist. *Europace.* 2009; 11 (Suppl 5): v15–v21, doi: [10.1093/europace/eup270](https://doi.org/10.1093/europace/eup270), indexed in Pubmed: [19861386](https://pubmed.ncbi.nlm.nih.gov/19861386/).
7. Jongbloed MRM, Lamb HJ, Bax JJ, et al. Noninvasive visualization of the cardiac venous system using multislice computed tomography. *J Am Coll Cardiol.* 2005; 45(5): 749–753, doi: [10.1016/j.jacc.2004.11.035](https://doi.org/10.1016/j.jacc.2004.11.035), indexed in Pubmed: [15734621](https://pubmed.ncbi.nlm.nih.gov/15734621/).
8. Kassem M, Lake S, Roberts W, et al. Cardiac veins, an anatomical review. *Transl Res Anat.* 2021; 23: 100096, doi: [10.1016/j.tria.2020.100096](https://doi.org/10.1016/j.tria.2020.100096).
9. Khan FZ, Virdee MS, Gopalan D, et al. Characterization of the suitability of coronary venous anatomy for targeting left ventricular lead placement in patients undergoing cardiac resynchronization therapy. *Europace.* 2009; 11(11): 1491–1495, doi: [10.1093/europace/eup292](https://doi.org/10.1093/europace/eup292), indexed in Pubmed: [19880411](https://pubmed.ncbi.nlm.nih.gov/19880411/).
10. Kozłowski D, Koźluk E, Piatkowska A, et al. The middle cardiac vein as a key for “posteroseptal” space: a morphological point of view. *Folia Morphol.* 2001; 60(4): 293–296, indexed in Pubmed: [11770339](https://pubmed.ncbi.nlm.nih.gov/11770339/).
11. Manolis AS. Transseptal access to the left atrium: tips and tricks to keep it safe derived from single operator experience and review of the literature. *Curr Cardiol Rev.* 2017; 13(4): 305–318, doi: [10.2174/1573403X13666170927122036](https://doi.org/10.2174/1573403X13666170927122036), indexed in Pubmed: [28969539](https://pubmed.ncbi.nlm.nih.gov/28969539/).
12. Markstad H, Bakos Z, Ostenfeld E, et al. Preoperative CT of cardiac veins for planning left ventricular lead placement in cardiac resynchronization therapy. *Acta Radiol.* 2019; 60(7): 859–865, doi: [10.1177/0284185118803796](https://doi.org/10.1177/0284185118803796), indexed in Pubmed: [30304945](https://pubmed.ncbi.nlm.nih.gov/30304945/).
13. Mazur M, Hołda M, Koziej M, et al. Morphology of tributaries of coronary sinus in humans — corrosion casting study. *Folia Med Cracov.* 2015; 55(2): 5–13, indexed in Pubmed: [26839238](https://pubmed.ncbi.nlm.nih.gov/26839238/).
14. Mazur M, Tomaszewska R, Pasternak A, et al. The Thebesian valve and its significance for electrophysiologists. *Folia Morphol.* 2014; 73(3): 298–301, doi: [10.5603/FM.2014.0047](https://doi.org/10.5603/FM.2014.0047), indexed in Pubmed: [25242157](https://pubmed.ncbi.nlm.nih.gov/25242157/).
15. Młynarski R, Młynarska A, Gołba KS, et al. Visualisation of the oblique vein of the left atrium (vein of Marshall) using cardiac computed tomography: is the game worth the candle? *Kardiol Pol.* 2018; 76(9): 1344–1349, doi: [10.5603/KPa.2018.0131](https://doi.org/10.5603/KPa.2018.0131), indexed in Pubmed: [30251241](https://pubmed.ncbi.nlm.nih.gov/30251241/).
16. Noheria A, Sodhi S, Orme GJ. The evolving role of electrocardiography in cardiac resynchronization therapy. *Curr Treat Options Cardiovasc Med.* 2019; 21(12): 91, doi: [10.1007/s11936-019-0784-6](https://doi.org/10.1007/s11936-019-0784-6), indexed in Pubmed: [31828564](https://pubmed.ncbi.nlm.nih.gov/31828564/).
17. Ojo A, Tariq S, Harikrishnan P, et al. Cardiac resynchronization therapy for heart failure. *Interv Cardiol Clin.* 2017; 6(3): 417–426, doi: [10.1016/j.iccl.2017.03.010](https://doi.org/10.1016/j.iccl.2017.03.010), indexed in Pubmed: [28600094](https://pubmed.ncbi.nlm.nih.gov/28600094/).
18. Ortale JR, Gabriel EA, Iost C, et al. The anatomy of the coronary sinus and its tributaries. *Surg Radiol Anat.* 2001; 23(1): 15–21, doi: [10.1007/s00276-001-0015-0](https://doi.org/10.1007/s00276-001-0015-0), indexed in Pubmed: [11370136](https://pubmed.ncbi.nlm.nih.gov/11370136/).
19. Rad MM, Blaauw Y, Dinh T, et al. Left ventricular lead placement in the latest activated region guided by coronary venous electroanatomic mapping. *Europace.* 2015; 17(1): 84–93, doi: [10.1093/europace/euu221](https://doi.org/10.1093/europace/euu221), indexed in Pubmed: [25186457](https://pubmed.ncbi.nlm.nih.gov/25186457/).
20. Roberts W, Salandy S, Mandal G, et al. Across the centuries: piecing together the anatomy of the heart. *Transl Res Anat.* 2019; 17: 100051, doi: [10.1016/j.tria.2019.100051](https://doi.org/10.1016/j.tria.2019.100051).

21. Saremi F, Muresian H, Sánchez-Quintana D. Coronary veins: comprehensive CT-anatomic classification and review of variants and clinical implications. *Radiographics*. 2012; 32(1): E1–32, doi: [10.1148/rg.321115014](https://doi.org/10.1148/rg.321115014), indexed in Pubmed: [22236907](https://pubmed.ncbi.nlm.nih.gov/22236907/).
22. Shah SS, Teague SD, Lu JC, et al. Imaging of the coronary sinus: normal anatomy and congenital abnormalities. *Radiographics*. 2012; 32(4): 991–1008, doi: [10.1148/rg.324105220](https://doi.org/10.1148/rg.324105220), indexed in Pubmed: [22786990](https://pubmed.ncbi.nlm.nih.gov/22786990/).
23. Sinha M, Pandey NN, Sharma A. Anomalies of the coronary sinus and its tributaries: evaluation on multidetector computed tomography angiography. *J Thorac Imaging*. 2020; 35(2): W60–W67, doi: [10.1097/RTI.0000000000000456](https://doi.org/10.1097/RTI.0000000000000456), indexed in Pubmed: [31688460](https://pubmed.ncbi.nlm.nih.gov/31688460/).
24. Sirajuddin A, Chen MY, White CS, et al. Coronary venous anatomy and anomalies. *J Cardiovasc Comput Tomogr*. 2020; 14(1): 80–86, doi: [10.1016/j.jcct.2019.08.006](https://doi.org/10.1016/j.jcct.2019.08.006), indexed in Pubmed: [31444098](https://pubmed.ncbi.nlm.nih.gov/31444098/).
25. Sommer A, Kronborg MB, Nørgaard BL, et al. Left and right ventricular lead positions are imprecisely determined by fluoroscopy in cardiac resynchronization therapy: a comparison with cardiac computed tomography. *Europace*. 2014; 16(9): 1334–1341, doi: [10.1093/europace/euu056](https://doi.org/10.1093/europace/euu056), indexed in Pubmed: [24687965](https://pubmed.ncbi.nlm.nih.gov/24687965/).
26. von Lüdinghausen M. The venous drainage of the human myocardium. *Adv Anat Embryol Cell Biol*. 2003; 168: I–VIII, 1, doi: [10.1007/978-3-642-55623-4](https://doi.org/10.1007/978-3-642-55623-4), indexed in Pubmed: [12645157](https://pubmed.ncbi.nlm.nih.gov/12645157/).
27. von Lüdinghausen M. Clinical anatomy of cardiac veins, Vv. cardiaca. *Surg Radiol Anat*. 1987; 9(2): 159–168, doi: [10.1007/BF02086601](https://doi.org/10.1007/BF02086601), indexed in Pubmed: [3120334](https://pubmed.ncbi.nlm.nih.gov/3120334/).
28. Whiteman S, Saker E, Courant V, et al. An anatomical review of the left atrium. *Transl Res Anat*. 2019; 17: 100052, doi: [10.1016/j.tria.2019.100052](https://doi.org/10.1016/j.tria.2019.100052).
29. Wouters PC, van Everdingen WM, Vernooij K, et al. Does mechanical dyssynchrony in addition to QRS area ensure sustained response to cardiac resynchronization therapy? *Eur Heart J Cardiovasc Imaging*. 2022; 23(12): 1628–1635, doi: [10.1093/ehjci/jeab264](https://doi.org/10.1093/ehjci/jeab264), indexed in Pubmed: [34871385](https://pubmed.ncbi.nlm.nih.gov/34871385/).
30. Yaminisharif A, Davoodi G, Kazemisaeid A, et al. Characterization of suitability of coronary venous anatomy for targeting left ventricular lead placement in patients undergoing cardiac resynchronization therapy. *J Tehran Heart Cent*. 2012; 7(1): 10–14, indexed in Pubmed: [23074628](https://pubmed.ncbi.nlm.nih.gov/23074628/).
31. Żabówka A, Hołda J, Strona M, et al. Morphology of the Vieussens valve and its imaging in cardiac multislice computed tomography. *J Cardiovasc Electrophysiol*. 2019; 30(8): 1325–1329, doi: [10.1111/jce.14018](https://doi.org/10.1111/jce.14018), indexed in Pubmed: [31187551](https://pubmed.ncbi.nlm.nih.gov/31187551/).
32. Żabówka A, Jakiel M, Bolechała F, et al. Topography of the oblique vein of the left atrium (vein of Marshall). *Kardiol Pol*. 2020; 78(7-8): 688–693, doi: [10.33963/KP.15318](https://doi.org/10.33963/KP.15318), indexed in Pubmed: [32347083](https://pubmed.ncbi.nlm.nih.gov/32347083/).
33. Zhivadinovik J, Papazova M, Matveeva N, et al. Anatomy of coronary sinus ostium. *Folia Morphol*. 2016; 75(2): 264–267, doi: [10.5603/FM.a2015.0089](https://doi.org/10.5603/FM.a2015.0089), indexed in Pubmed: [26431050](https://pubmed.ncbi.nlm.nih.gov/26431050/).